The 2010 IEEE/RSJ International Conference on
Intelligent Robots and Systems
October 18-22, 2010, Taipei, Taiwan

Motion Planning and Control of an Underactuated 3DOF Helicopter

Simon Westerberg, Uwe Mettin, Anton Shiriaev

Abstract— **We consider trajectory planning for an underactuated 3DOF helicopter, using the virtual holonomic constraint approach. First we choose constraint functions that describe the configuration variables along a desired motion in terms of some independent parametrization variable. This lets us describe the closed-loop system by some reduced order dynamics, the solution of which gives a feasible trajectory for the desired motion. By using the method of transverse linearization for controller design, we achieve exponential orbital stability to a desired trajectory. Numerical simulations confirm this property and show good convergence to a desired periodic motion when initialized from a resting state.**

Index Terms— **Motion Planning and Control, Virtual Holonomic Constraints, Reduced Dynamics**

I. Introduction

Motion planning and stabilization of underactuated mechanical systems is a classical control problem. Applications can be found in control of surface vessels, underwater vehicles, spacecraft and aircraft, see e.g. [8], [2], [4] and references therein. Underactuation may appear from actuator failure in fully actuated systems or by design. In the first case, a control strategy for underactuated systems can be applied to still allow some motions to be carried out. The latter occurs when restrictions in cost, weight, size, or efficiency favors a smaller number of actuators.

An underactuated system with non-linear dynamics that presents interesting challenges in motion planning and control is the 3DOF helicopter developed by Quanser [9], shown in Fig. 1. The system has been used as experimental platform for evaluation of various control methods, e.g. robust predictive control [7], neural network-based adaptive control [3] and multiple-system motion synchronization [10].

The most typical approach to stabilization of motions in underactuated systems is to stabilize some integrals of motions present in the control-free system and corresponding to some natural rotations. The reason for such an approach is to avoid dealing with careful motion planning which is not trivial, since the lack of control inputs makes it impossible to prescribe arbitrary time-evolutions of the generalized coordinates. The restriction of the family of targeted motions to the natural ones may not allow achieving certain desired characteristics of the executed motions.

Our approach to motion planning is based on the idea of representing a desired trajectory in time-independent form, with the evolution of the generalized coordinates specified as geometric functions of some synchronization variable. We compute the reduced dynamics that describes possible dynamics along the path independent on the control signals. We then select a solution to the reduced dynamics that provides the specified motion with its desired characteristics.

Stabilization is done using a special coordinate transformation in a vicinity of the feasible trajectory, which is constructed using the synchronization function and a conserved quantity for the reduced dynamics.

The rest of the paper is organized as follows. The dynamical model of the 3DOF helicopter is introduced in Section II. In Section III we describe the virtual holonomic constraint approach to motion planning and how a trajectory is obtained from reduced order dynamics. This is illustrated with three periodic motions of different complexity. Section IV presents the design of a controller based on transverse linearization, as well as results from numerical simulations. The paper ends with concluding remarks.

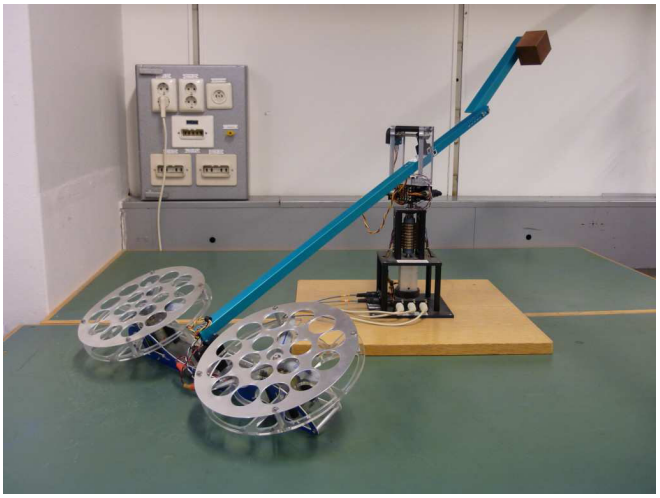

Fig. 1. The 3DOF helicopter setup by Quanser [9].

II. Dynamic Model

The model we consider is a 3DOF helicopter produced by Quanser [9], as shown in Fig. 1. The helicopter is a rigid body attached with a spherical joint at a suspension point, around which it can rotate freely in any direction. It has two control inputs in the form of individually controlled rotors, leaving one degree of freedom unactuated. The rotors are symmetrically attached at one side of the body. At the opposite end, a counterweight is attached to reduce the effect of the gravitational forces.

The authors are with the Department of Applied Physics and Electronics, Umeå University, SE-901 87 Umeå, Sweden. E-mail: simon.westerberg@tfe.umu.se.

U. Mettin and A. Shiriaev are also with the Department of Engineering Cybernetics, Norwegian University of Science and Technology, NO-7491 Trondheim, Norway.

The dynamics of the helicopter can be modeled using the Newton-Euler equation[14]:

$$I\dot{\omega} + \omega \times (I\omega) = \tau, \tag{1}$$

where $\omega = [\omega_x, \omega_y, \omega_z]^T$ is the angular velocity, $I = \mathrm{diag}(I_x, I_y, I_z)$ is the inertia matrix for the rigid body and $\tau = [\tau_x, \tau_y, \tau_z]^T$ is the total amount of torques acting on the body. Note that all of these variables are expressed in the body attached frame. We use Z-Y-X Euler angles $q = [\psi, \theta, \phi]^T$ as generalized coordinates for the orientation of the rigid body. They describe consecutive rotations about the current body axis, also known as yaw-pitch-roll transformation. A graphical description of the generalized coordinates of the 3DOF helicopter model is shown in Fig. 2.

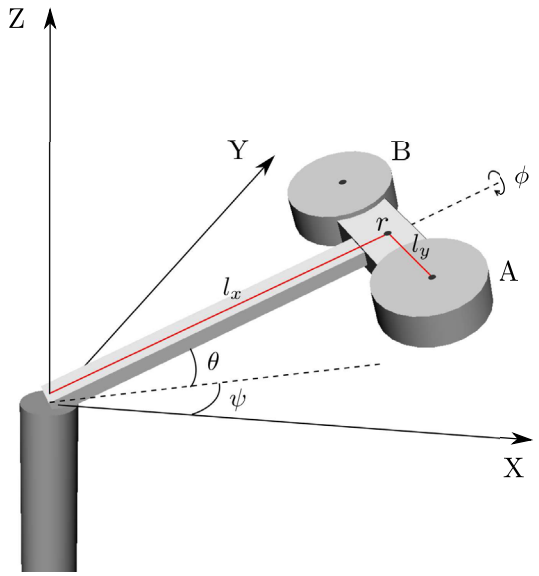

Fig. 2. Graphical representation of the generalized coordinates of the 3DOF helicopter model.

The transformation of a vector from the body attached frame to the inertial frame is performed by multiplication with the following rotation matrix

$$\begin{aligned} R &= R_{z,\psi} R_{y,\theta} R_{x,\phi} \\ &= \begin{bmatrix} c_\psi c_\theta & c_\psi s_\theta s_\phi - s_\psi c_\phi & c_\psi s_\theta c_\phi + s_\psi s_\phi \\ s_\psi c_\theta & s_\psi s_\theta s_\phi + c_\psi c_\phi & s_\psi s_\theta c_\phi - c_\psi s_\phi \\ -s_\theta & c_\theta s_\phi & c_\theta c_\phi \end{bmatrix}, \end{aligned} \tag{2}$$

where $c_\cdot$ and $s_\cdot$ denote $\cos(\cdot)$ and $\sin(\cdot)$ respectively. The columns of the matrix R specify the axes of the body attached frame, in which the elements in (1) are expressed.

The angular velocity expressed in the fixed inertia frame, ω_I, is related to the rates of change of the individual elements of q as

$$\omega_I = B_{zyx}\,\dot{q} = \begin{bmatrix} 0 & -s_\psi & c_\psi c_\theta \\ 0 & c_\psi & s_\psi c_\theta \\ 1 & 0 & -s_\theta \end{bmatrix} \begin{bmatrix} \dot{\psi} \\ \dot{\theta} \\ \dot{\phi} \end{bmatrix} \tag{3}$$

In body frame the angular velocity ω can be expressed as

$$\omega = R^T \omega_I = R^T B_{zyx}(q)\dot{q}. \tag{4}$$

The dynamical model is simplified by not taking air resistance or friction into account. Thus, the torque τ can be divided into two components, $\tau = \tau_u + \tau_g$, where τ_g is the torque introduced by the gravitational force and τ_u is the vector of controlled torques. Let $r = [l_x, 0, 0]^T$ be the center point between the two rotors. We introduce the vector $\Gamma = [\Gamma_x, \Gamma_y, \Gamma_z]^T$ as the vector of gravitational force, acting on the point r, expressed in body frame coordinates, i.e.

$$\Gamma = R^T \begin{bmatrix} 0 \\ 0 \\ -mg \end{bmatrix} \tag{5}$$

where m is the effective mass at r, and g is the gravitational constant. The torque τ_g can now be calculated as

$$\tau_g = r \times \Gamma = \begin{bmatrix} 0 \\ l_x \Gamma_z \\ l_x \Gamma_y \end{bmatrix}. \tag{6}$$

The body is not actuated about the yaw-axis making the vector of controlled torques to be

$$\tau_u = [\tau_{u_x}, \tau_{u_y}, 0]^T, \tag{7}$$

so the 3DOF helicopter described above is of underactuation degree one.

The forces that need to be applied at each rotor in order to induce the torques in (7) are

$$F_A = -\frac{1}{2}\left(\frac{\tau_{u_x}}{l_y} + \frac{\tau_{u_y}}{l_x}\right), F_B = \frac{1}{2}\left(\frac{\tau_{u_x}}{l_y} - \frac{\tau_{u_y}}{l_x}\right). \tag{8}$$

The physical model parameters for the 3DOF helicopter setup are listed in Table I, along with some constraints of the configuration space as well as limitations on the available control forces.

TABLE I

PARAMETERS AND CONSTRAINTS OF THE 3DOF HELICOPTER.

Parameters	Values
Inertias [kg m^2]	$I_x = 0.042, I_y = 1.203, I_z = 1.203$
Lengths [m]	$l_x = 0.67$
	$l_y = 0.177$
Effective mass at r [kg]	$m = 0.127$
Gravitational constant [m/s^2]	$g = 9.81$
Position constraints [rad]	$\psi \in [-\inf, \inf]$
	$\theta \in [-0.6, 0.39]$
	$\phi \in [-\pi/2, \pi/2]$
Force constraints [Nm]	$F_A \in [0, 2.1]$
	$F_B \in [0, 2.1]$

III. MOTION PLANNING

A. Concept of Virtual Holonomic Constraints and Reduced Dynamics

The virtual holonomic constraints approach is a generic tool for motion planning and control, especially for underactuated systems. The main idea is to parametrize feasible motions by a geometric function of the generalized coordinates defining their synchronization [1]. If this function is preserved by some control action along solutions of

the closed-loop system, it is called a *virtual holonomic (geometric) constraint* [12], [15].

We choose to illustrate this approach for the helicopter model (1)–(4) by planning some motions about the yaw axis. We also incorporate additional desired characteristics of the motions into the motion planning process by constraining the motions to be periodic. An alternative restriction could e.g. be a desired completion time of the motion.

Let us chose the coordinate ψ as an independent variable used to parameterize such a motion. The other two generalized coordinates shall be geometrically related to ψ, such that a path is determined in the configuration space. Hence, the virtual holonomic constraint takes the form

$$q = \begin{bmatrix} \psi \\ \theta \\ \phi \end{bmatrix} := F(\psi) = \begin{bmatrix} \psi \\ f_1(\psi) \\ f_2(\psi) \end{bmatrix} . \tag{9}$$

Note that the function (9) can be derived either by observation of some real motion, by analytical design procedures, or by some numerical search.

Suppose that there exists a control law $\tau_u = \tau_\star(t)$ for the controlled input torque τ_u of the underactuated system (1)–(4) that makes the virtual holonomic constraint (9) invariant. Then, the overall closed-loop system can be represented by the reduced order dynamics of the form [13], [11]

$$\alpha(\psi)\,\ddot{\psi} + \beta(\psi)\,\dot{\psi}^2 + \gamma(\psi) = 0\,. \tag{10}$$

The solutions of this virtually constrained system define achievable motions of the body with precise synchronization given by (9). It means that the whole motion is parameterized by the evolution of the chosen configuration variable ψ. The smooth functions $\alpha(\psi)$, $\beta(\psi)$ and $\gamma(\psi)$ are given in Table II.

It is important to observe that the reduced order dynamics (10) is always integrable, provided $\alpha(\theta) \neq 0$. Specifically, the integral function [11], [13]

$$\begin{aligned} I(\psi,\dot{\psi},\psi_0,\dot{\psi}_0) \;&=\; \dot{\psi}^2 - \exp\left\{-2\int_{\psi_0}^{\psi}\frac{\beta(\tau)}{\alpha(\tau)}\,d\tau\right\}\dot{\psi}_0^2 \\ &+ \int_{\psi_0}^{\psi}\exp\left\{-2\int_{s}^{\psi}\frac{\beta(\tau)}{\alpha(\tau)}\,d\tau\right\}\frac{2\,\gamma(s)}{\alpha(s)}\,ds \end{aligned} \tag{11}$$

preserves its zero value along the solution of (10), initiated at $(\psi(0),\dot{\psi}(0)) = (\psi_0,\dot{\psi}_0)$. Note that (11) can serve as a measure of distance to a desired trajectory [11].

Eventually, one can also compute the nominal control input $\tau_\star$ required to generate a desired solution $\psi = \psi_\star(t)$ of (10) assuming perfectly imposed virtual holonomic constraints (9):

$$\tau_* = \begin{bmatrix} 1 & 0 & 0 \\ 0 & 1 & 0 \end{bmatrix} [I\dot{\omega} + \omega \times (I\omega) - \tau_g]\Big|_{\substack{q = F(\psi_*) \\ \dot{q} = F'(\psi_*)\dot{\psi}_* \\ \ddot{q} = F''(\psi_*)\dot{\psi}_*^2 \\ \qquad + F'(\psi_*)\ddot{\psi}_*}} \tag{12}$$

In the following sections we illustrate the approach of using virtual holonomic constraints for motion planning of the 3DOF helicopter, applied to three periodic motions of different complexity.

B. Motion 1: constant pitch and roll

The first motion we consider is the simple case of periodicity about the yaw axis, where roll and pitch are constant, described by the following virtual holonomic constraint

$$\begin{aligned} \theta &= f_1(\psi) \equiv c_1\,, \\ \phi &= f_2(\psi) \equiv c_2\,. \end{aligned} \tag{13}$$

By substituting (13) into the functions of Table II, we get the following expressions for reduced dynamics coefficients:

$$\begin{aligned} \alpha(\psi) &= I_z\cos(c_1)\cos(c_2)\,, \\ \beta(\psi) &= (I_x - I_y)\sin(c_1)\sin(c_2)\cos(c_1)\,, \\ \gamma(\psi) &= mgl_x\cos(c_1)\sin(c_2)\,. \end{aligned} \tag{14}$$

Due to the influence of gravity, we cannot always expect periodicity for the trajectories that are obtained as solutions to (10) even if the constraint functions are periodic. For simplicity, assume that $c_1 = 0$. By substituting (14) into the integral function (11) it can be derived that

$$\dot{\psi} = \sqrt{\dot{\psi}_0^2 - \frac{2ml_x g\sin(c_2)\psi}{I_z cos(c_2)}}. \tag{15}$$

along the trajectory, given some initial velocity $\dot{\psi}(0) = \dot{\psi}_0$. Periodicity in our case implies that $\dot{\psi}(2n\pi) = \dot{\psi}(0)$ for any $n \in 1, 2, 3, ...$ This motion is thus only periodic provided that $c_2 = 0$, i.e. when the gravity torque vector τ_g and the controlled input torque vector τ_u are parallel. In this case the velocity will be constant during the motion. If $c_2 < 0$, however, the counteracting force from the rotors includes a component that is perpendicular to the gravity vector Γ and thereby adds to the energy of the system by increasing the velocity $\dot{\psi}$. Conversely, if $c_2 > 0$, energy will be dissipated from the system.

C. Motion 2: cyclic pitch, constant roll

As a second example we consider a more complicated motion where the pitch (θ) is described by a cyclic function while the roll (ϕ) is kept constant. This can be achieved by constructing the following virtual constraint

$$\begin{aligned} \theta &= f_1(\psi) \equiv c_1 \cdot cos(n \cdot \psi)\,, \\ \phi &= f_2(\psi) \equiv c_2\,. \end{aligned} \tag{16}$$

As with our first motion, we only achieve periodicity when $c_2 = 0$. We hence choose the parameters $c_1 = 0.25$, $c_2 = 0$, with $n = 4$, and select the following trajectory for the path given by (16):

$$\begin{aligned} &\psi_*(t) \in [0,\ 2\pi]\,\text{rad}\,, \\ &\text{for } t \in [0,\ T] \text{ with } T = 16.21\,\text{s}\,, \text{ and} \\ &(\psi_*(0),\dot{\psi}_*(0)) = (0\,\text{rad},\ 0.4\,\text{rad/s}) \end{aligned} \tag{17}$$

which gives the following scalar coefficient functions for the reduced dynamics

$$\begin{aligned} \alpha(\psi) &= I_z\cos(c_1\cos(n\psi))\,, \\ \beta(\psi) &= -c_1 n(I_x - I_y - I_z)\sin(n\psi)\sin(c_1\cos(n\psi))\,, \\ \gamma(\psi) &= 0\,. \end{aligned} \tag{18}$$

The fact that $\gamma = 0$ implies that the reduced dynamics is not influenced by gravity and the solution (trajectory) to (10) is

TABLE II

SCALAR COEFFICIENT FUNCTIONS OF THE REDUCED DYNAMICS (10).

$$
\begin{aligned}
\alpha(\psi) &= I_z(\cos(f_1(\psi))\cos(f_2(\psi)) - f_1'(\psi)\sin(f_2(\psi)))\\
\beta(\psi) &= -I_z\sin(f_2(\psi))f_1''(\psi) + ((I_y - I_z - I_x)f_2'(\psi) + \sin(f_1(\psi))(I_x - I_z - I_y))\cos(f_2(\psi))f_1'(\psi) +\\
&\quad ((I_y - I_z - I_x)f_2'(\psi) + \sin(f_1(\psi))(-I_y + I_x))\cos(f_1(\psi))\sin(f_2(\psi))\\
\gamma(\psi) &= mgl_x\cos(f_1(\psi))\sin(f_2(\psi))
\end{aligned}
$$

identical to a solution for the rotating body in gravity-free conditions. The trajectory corresponding to this solution is shown in Fig. 3. However, the full dynamics (1) is affected by the gravity and corresponding terms still appear in the torques required for compliance to the trajectory. Gravity shifts the torque away from a zero mean. Individual rotor forces are shown in Fig. 4.

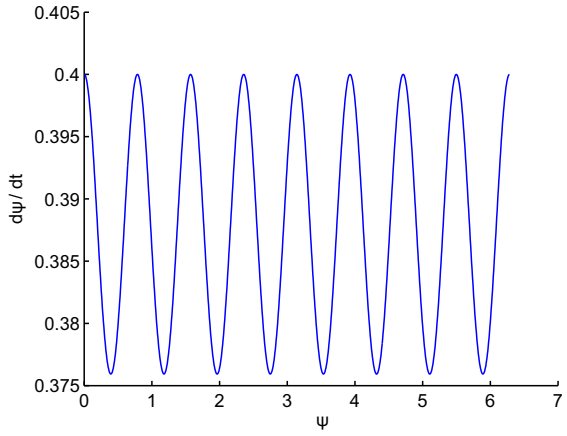

Fig. 3. Velocity profile for the trajectory of the second motion, parametrized by (16).

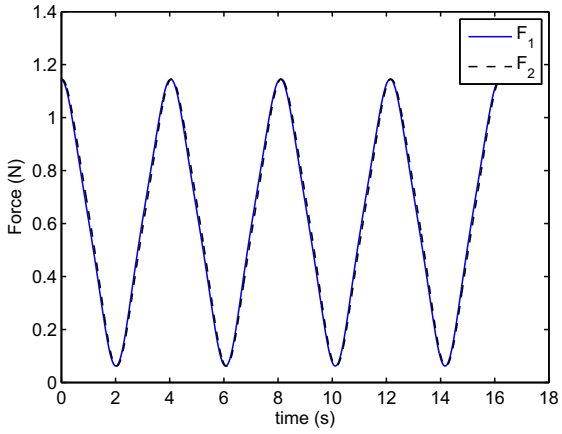

Fig. 4. Required individual rotor forces for motion 2.

D. Motion 3: constant pitch, cyclic roll

For our third motion, we let the pitch be constant while varying the roll in a cyclic fashion, by choosing the virtual constraint function as

$$
\begin{aligned}
\theta &= f_1(\psi) \equiv c_1\\
\phi &= f_2(\psi) \equiv c_2 \cdot cos(n \cdot \psi)
\end{aligned}
\tag{19}
$$

with the parameters $c_1 = 0$, $c_2 = 0.5$, and $n = 4$. Along the path specified by (19), we select the following trajectory:

$$
\begin{aligned}
&\psi_*(t) \in [0,\ 2\pi]\,\text{rad}\,,\\
&\text{for } t \in [0,\ T] \text{ with } T = 14.55\,\text{s}\,, \text{ and}\\
&(\psi_*(0), \dot{\psi}_*(0)) = (0\,\text{rad},\ 0.5\,\text{rad/s})
\end{aligned}
\tag{20}
$$

The scalar coefficient functions for the reduced dynamics become

$$
\begin{aligned}
\alpha(\psi) &= I_z\cos(c_1)\cos(c_2\cos(n\psi))\\
\beta(\psi) &= (nc_2(I_x + I_z - I_y)\sin(n\psi) + \sin(c_1)(I_x - I_y))\cdot\\
&\quad \sin(c_2\cos(n\psi))\cos(c_1)\\
\gamma(\psi) &= mgl_x\cos(c_1)\sin(c_2\cos(n\psi))
\end{aligned}
\tag{21}
$$

and its solution gives a trajectory with the velocity profile as shown in Fig. 5. The time evolution of this trajectory can be seen in Fig. 6. The forces required from the rotors during the motion are shown in Fig 7.

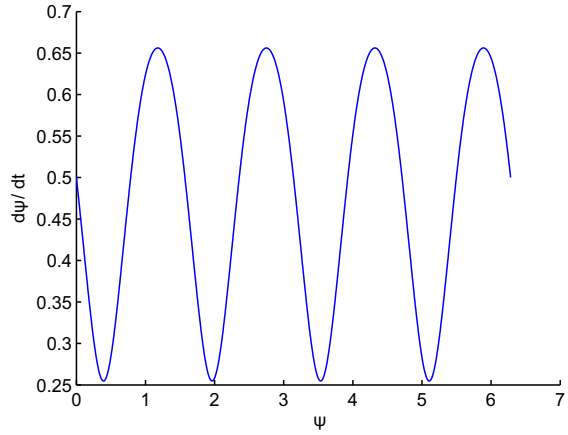

Fig. 5. Velocity profile for the trajectory of the third motion, parametrized by (19).

IV. CONTROLLER DESIGN

The design step following the motion planning is the synthesis of a feedback controller with the objective to achieve exponential orbital stability to the desired trajectory and to diminish effects of disturbances, uncertainties in modeling, errors in parameter estimates, etc. Here, we show a controller design based on a transverse linearization [11] of the system dynamics along the desired trajectory.

At first, let us introduce new independent coordinates for the 3DOF rigid body (1)–(4):

$$
y = \begin{bmatrix} \theta - f_1(\psi) \\ \phi - f_2(\psi) \end{bmatrix} \quad \text{and} \quad \psi\,,
\tag{22}
$$

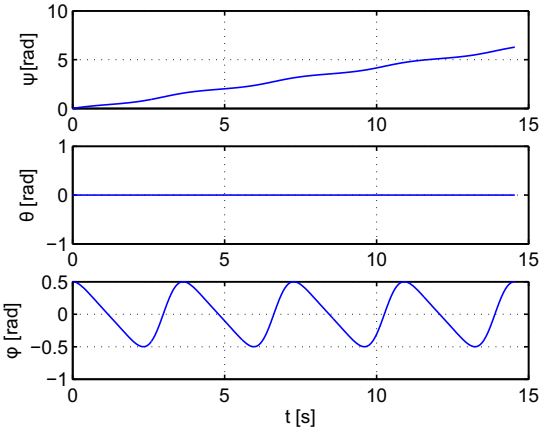

Fig. 6. Time evolution of the generalized coordinates for the trajectory of the third motion.

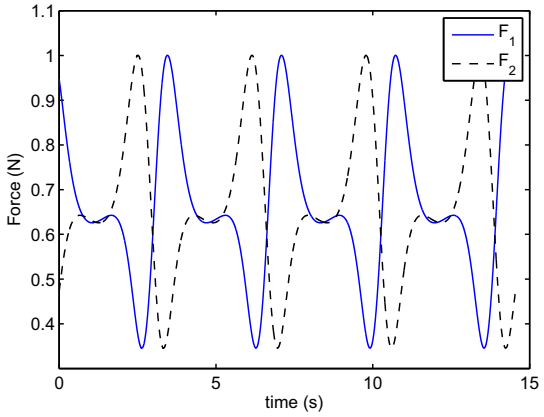

Fig. 7. Required individual rotor forces for motion 3.

where y gives the synchronization error for the virtual holonomic constraints defined by (9). It is clear that the first and second time derivatives of y and ψ are related to the original coordinates q and their time derivatives. With the change of generalized coordinates (22), the dynamics of y takes the form

$$\ddot{y} = R(y, \psi, \dot{y}, \dot{\psi}) + N(y, \psi)\,\tau = v\,,$$

where v is introduced as a virtual control input that is used for stabilization of a preplanned trajectory. The feedback transformation[1]

$$\tau = N^{-1}(y, \theta)\left[v - R(y, \theta, \dot{y}, \dot{\theta})\right] \tag{23}$$

associates v with the corresponding input torque τ. For perfectly invariant constraints $q = F(\psi_\star)$, $\dot{q} = F(\psi_\star)\dot{\psi}_\star$, the virtual control variable v is zero and (23) gives the nominal torque (12). As shown in [12], [11], in the new coordinates the dynamics of the system is given in partly linear form:

$$\begin{aligned}\alpha(\psi)\ddot{\psi}+\beta(\psi)\dot{\psi}^2+\gamma(\psi) &= g_y(\psi,\dot{\psi},\ddot{\psi},y,\dot{y})y+\\ &\quad +g_{\dot{y}}(\psi,\dot{\psi},\ddot{\psi},y,\dot{y})\dot{y}+g_v(\psi,\dot{\psi},y,\dot{y})v\\ \ddot{y} &= v\,,\end{aligned}$$

[1]We check that the matrix N is non-singular in the vicinity of our preplanned motions.

where the left-hand side of the upper equation corresponds to the one for the virtually constrained system (10), while the right-hand side is rewritten in the new coordinates (22) and is equal to zero along the target motion.

With the reduced dynamics (10) being integrable, we can define dynamics transversal to the solution as follows:

$$\begin{aligned}\tfrac{d}{dt}I(\cdot) &= \tfrac{2\dot{\psi}}{\alpha(\psi)}\left[g_y(\cdot)y + g_{\dot{y}}(\cdot)\dot{y} + g_v(\cdot)v - \beta(\psi)I(\cdot)\right]\\ \ddot{y} &= v\,.\end{aligned} \tag{24}$$

Thus, the transverse coordinates for a given trajectory are

$$x_\perp = \left[I\left(\psi, \dot{\psi}, \psi_\star(0), \dot{\psi}_\star(0)\right),\, y^T,\, \dot{y}^T\right]^T$$

with dimension $2n-1$, where $n = \dim q$. Eventually, the controller design can be based on the linearization of the transverse dynamics (24) along a desired solution $\psi_\star(t)$—a linear time-variant comparison system called transverse linearization given in the form [11]:

$$\begin{aligned}\tfrac{d}{dt}z &= A(\psi_\star(t), \dot{\psi}_\star(t))z + B(\psi_\star(t), \dot{\psi}_\star(t))w\\ z &= [\delta I, \delta y, \delta\dot{y}]^\tau\,.\end{aligned} \tag{25}$$

Exponential orbital feedback stabilization within a vicinity of the desired trajectory can be achieved by using $w = -\Gamma^{-1}B(t)^T R(t)z$, where R is a solution of the continuous time-periodic matrix Riccati equation

$$\dot{R}(t)+A(t)^T R(t)+R(t)A(t)+Q = R(t)B(t)\Gamma^{-1}B(t)^T R(t)$$

with appropriately chosen weighting matrices $Q \geq 0$ and $\Gamma > 0$. This method used to find this solution is presented in [5], [6]. The explicit dependence of time is removed by an operator that relates a point in the phase plane $(\psi, \dot{\psi})$ to the desired trajectory such that the corresponding stabilizing solution $R(t)$ can be used in the control law for the nonlinear system, see [11] for details. It should be also noted that one can often find a constant feedback gain that provides acceptable rate of convergence.

A. Simulation Results

In order to illustrate the exponential convergence properties of a transverse linearization based controller, we performed numerical simulations with a constant feedback gain designed for the third motion, i.e. constant pitch and cyclic roll, parametrized by (19)–(20). The system dynamics were initialized at a considerable distance away from the desired trajectory. The elements of the initial state vector $x(0) = [q(0), \dot{q}(0)]^T$ were chosen as

$$\begin{aligned}q(0) &= [0, 0.5, 0] = [\psi_\star(0), \theta_\star(0) + 0.5, \phi_\star(0) - 0.5]\\ \dot{q}(0) &= [0, 0, 0] \quad = [\dot{\psi}_\star(0) - 0.5, \dot{\theta}_\star(0), \dot{\phi}_\star(0)]\,,\end{aligned} \tag{26}$$

which corresponds to the helicopter being positioned at a resting state on the table. As can be seen in Fig. 8, the controller manages to recover the preplanned motion after some time, compare Fig. 6. Fig. 9 shows the velocity profile of the resulting trajectory, with initial conditions at $\psi = 0, \dot{\psi} = 0$, as stated by (26), showing convergence to the trajectory of Fig 5. Another measure of the performance of the controller can be seen in Fig. 10, which shows the vector norm of the transverse coordinates $x_\perp$ over time.

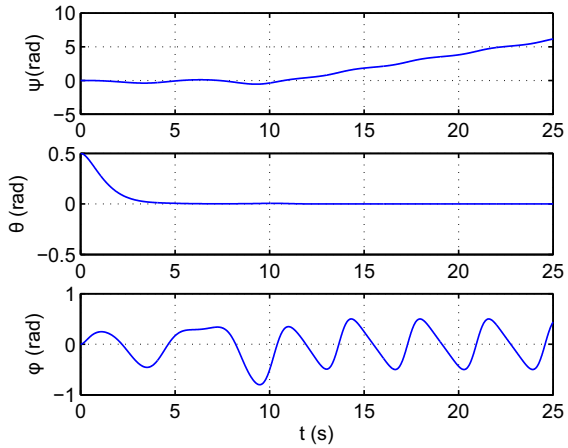

Fig. 8. Time evolution of the simulated closed loop system.

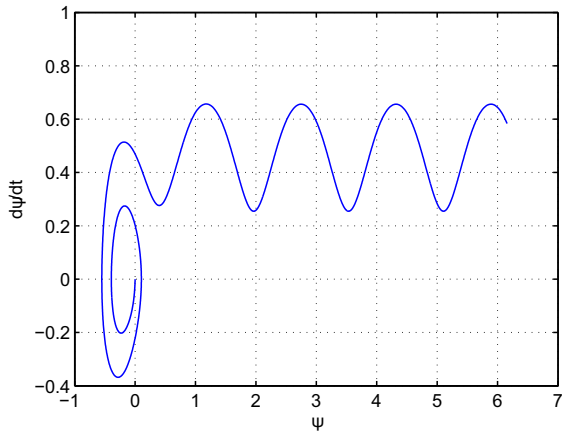

Fig. 9. Phase space trajectory for closed loop simulation, initiated at $\psi = 0, \dot{\psi} = 0$, showing convergence to the preplanned periodic trajectory.

V. Conclusions

We have considered the problem of trajectory planning for an underactuated 3DOF helicopter. We used the concept of virtual holonomic constraints to plan feasible motions. The procedure was illustrated by the planning of different motions about the yaw axis, using the yaw configuration variable as parametrization. By selecting a certain solution to the reduced dynamics, the motions were designed to be periodic. The range of motions feasible to plan with this approach is however not in any way limited to this class of motions.

A controller was designed for one of the periodic motions. Numerical simulations using the resulting controller show convergence to the preplanned motion, even when initialized at a resting position away from the trajectory, without violating position or force constraints.

We are currently in the process of conducting experiments on a physical setup, in order to practically validate our results. A further interesting extension to the current problem would be to apply this approach to a more complex helicopter system with additional translational degrees-of-freedom.

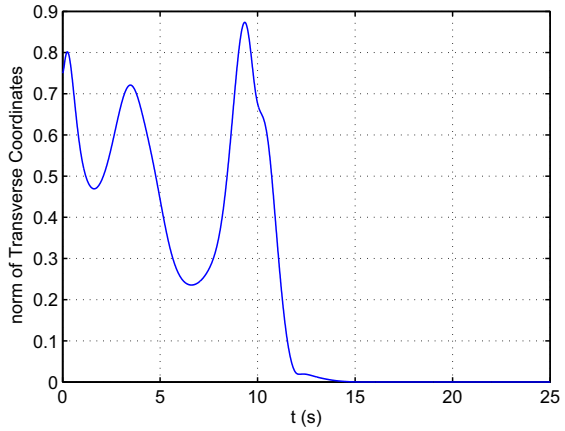

Fig. 10. Controller performance in simulation of the closed-loop system initialized away from the trajectory. The norm of the vector of transverse coordinates $x_\perp$ is shown.

References

[1] Y. Aoustin and A. Formal'sky, "Design of reference trajectory to stabilize desired nominal cyclic gait of a biped," in *Proceedings of the International Workshop on Robot Motion and Control, RoMoCo '99*, Kiekrz, Poland, June 1999.

[2] J.-M. Coron and E.-Y. Keraï, "Explicit feedbacks stabilizing the attitude of a rigid spacecraft with two control torques," *Automatica*, vol. 32, no. 5, pp. 669–677, 1996.

[3] F. G. M. de Carvalho and E. M. Hemerly, "Adaptive elevation control of a three degrees-of-freedom model helicopter using neural networks by state and output feedback," *ABCM Symposium Series in Mechatronics*, vol. 3, pp. 106–113, 2008.

[4] E. Frazzoli, M. A. Dahleh, and E. Feron, "Trajectory tracking control design for autonomous helicopters using a backstepping algorithm," in *Proceedings of the 2000 American Control Conference*, 2000, pp. 4102–4107.

[5] S. Gusev, S. Johansson, B. Kågström, A. S. Shiriaev, and A. Varga, "Numerical evaluation of solvers for the periodic Riccati differential equation," *BIT Numerical Mathematics*, 2010.

[6] S. Gusev, A. S. Shiriaev, and L. Freidovich, "LMI approach for solving periodic matrix Riccati equation," in *Proceedings of the 3rd IFAC workshop on Periodic Control Systems (PSYCO)*, 2007.

[7] M. H. Maia and R. K. H. G. ao, "Robust constrained predictive control of a 3dof helicopter model with external disturbances," *ABCM Symposium Series in Mechatronics*, vol. 3, pp. 19–26, 2008.

[8] K. Y. Pettersen and N. H., "Underactuated ship tracking control: theory and experiments," *International Journal of Control*, vol. 74, pp. 1435–1446, 2001.

[9] Quanser, "Quanser," URL: `http://www.quanser.com`, accessed on 2010-03-09.

[10] J. Shan, H.-T. Liu, and S. Nowotny, "Synchronised trajectory-tracking control of multiple 3-DOF experimental helicopters," *IEEE Proceedings - Control Theory and Applications*, vol. 152, no. 6, pp. 683–692, 2005.

[11] A. Shiriaev, L. Freidovich, and I. Manchester, "Can we make a robot ballerina perform a pirouette? Orbital stabilization of periodic motions of underactuated mechanical systems," *Annual Reviews in Control*, vol. 32, no. 2, pp. 200–211, 2008.

[12] A. Shiriaev, J. Perram, and C. Canudas-de-Wit, "Constructive tool for orbital stabilization of underactuated nonlinear systems: Virtual constraints approach," *IEEE Transactions on Automatic Control*, vol. 50, no. 8, pp. 1164–1176, 2005.

[13] A. Shiriaev, J. Perram, A. Robertsson, and A. Sandberg, "Periodic motion planning for virtually constrained Euler–Lagrange systems," *Systems and Control Letters*, vol. 55, pp. 900–907, 2006.

[14] M. Spong, S. Hutchinson, and M. Vidyasagar, *Robot Modeling and Control*. New Jersey: John Wiley and Sons, 2006.

[15] E. Westervelt, J. Grizzle, C. Chevallereau, J. Choi, and B. Morris, *Feedback Control of Dynamic Bipedal Robot Locomotion*. CRC Press, Taylor and Francis Group, 2007.